



Article

Morpholine-Modified Pd/ γ -Al₂O₃@ASMA Pellet Catalyst with Excellent Catalytic Selectivity in the Hydrogenation of *p*-Chloronitrobenzene to *p*-Chloroaniline

Wei Wang ^{1,†} , Wenlong Xu ^{2,†}, Kedar Bahadur Thapa ² , Xiaorui Yang ¹, Jinhua Liang ¹, Liyan Zhu ¹ and Jianliang Zhu ^{1,*}

¹ College of Biotechnology and Pharmaceutical Engineering, Nanjing Tech University (Nanjing Tech), 30 South Puzhu Road, Nanjing 211816, China; wangwei007@njtech.edu.cn (W.W.); yangxiaorui@njtech.edu.cn (X.Y.); jhliang@njtech.edu.cn (J.L.); 981314549@njtech.edu.cn (L.Z.)

² Key Laboratory of Flexible Electronics (KLOFE) & Institute of Advanced Materials (IAM), Jiangsu National Synergetic Innovation Center for Advanced Materials (SICAM), Nanjing Tech University (Nanjing Tech), 30 South Puzhu Road, Nanjing 211816, China; constantinos@njtech.edu.cn (W.X.); iamthapa@njtech.edu.cn (K.B.T.)

* Correspondence: jlzhu@njtech.edu.cn; Tel.: +86-139-0516-2748

† These authors contributed equally to this work.

Received: 6 September 2017; Accepted: 30 September 2017; Published: 30 September 2017

Abstract: An amino poly (styrene-*co*-maleic anhydride) polymer (ASMA) encapsulated γ -Al₂O₃ pellet material has been synthesized successfully. After loading with Pd species and modified with morpholine, the inorganic-organic hybrid material shows an excellent catalytic property in the selective hydrogenation of *p*-chloronitrobenzene (*p*-CNB) to *p*-chloroaniline (*p*-CAN). In this procedure, morpholine can connect with the polymer layer in a form of amide bond and acts as an unparalleled immobilized dechlorination inhibitor, which can avoid further dechlorination efficiently and keeps stability due to the repulsive effect from the surviving C-O-C bond. The catalyst as prepared was characterized by using XRD, TGA, SEM, TEM, FT-IR, and ICP-OES, and it was further tested in the selective hydrogenation of *p*-CNB. It shows a supreme catalytic activity (almost 100%) and selectivity (up to 99.51%) after recycling for even 10 times, much superior to the blank alumina supported palladium (47.09%).

Keywords: organic-inorganic hybrid; palladium catalyst; hydrogenation; dechlorination; *p*-chloroaniline

1. Introduction

Para-chloroaniline (*p*-CAN), one of the most important chemical intermediates, is widely used in dyes, preservatives, herbicides, pesticides, etc. [1,2]. Conventional methodologies based on the Béchamp reaction are currently obsolete due to the generation of toxic wastes in the process [3]. To protect the environment, the best way to synthesize *p*-CAN is the direct hydrogenation of para-chloronitrobenzene (*p*-CNB). However, in the process of *p*-CNB hydrogenation, dehalogenation cannot be easily avoided [4]. During the reaction, the reduction of the nitro group is a nucleophilic substitution process, while the hydrogenolysis of halogenated aromatic proportion is an electrophilic substitution reaction (Figure 1) [5]. Hydrogenolysis of the carbon-halogen bond is enhanced by the substitution of the amino group in the aromatic rings [6]. Many metal catalysts, such as Pt [7], Pd [8,9], Ru [10], and Ni [11,12], are used in this reaction. On one hand, Raney nickel is widely used in this hydrogenation reaction [11,12], but considering the selectivity, it is necessary to add an

electron-donating compound such as morpholine as an inhibitor [4]. On the other hand, the high cost of noble metals may reduce the large-scale application of this technology. In recent years, nano-materials have been broadly investigated in catalysis [13]. Among these new materials, nanoparticle palladium catalysts have a larger specific surface area, and they have a stronger adsorption capacity than metal Pd bulk in catalytic hydrogenation. This advantage can effectively improve the adsorption and conversion of reactants [14]. Nevertheless, under the single-component palladium catalyst, the selectivity of halogenated aromatic amines is unsatisfactory because of the unavoidable dehalogenation [15]. Therefore, the palladium metal catalyst needs to be treated with different strategies such as the addition of a second co-catalyst additive [16,17], being immobilized on metal oxide support [16] or polymers, which can affect the inhibition of dehalogenation [18,19].

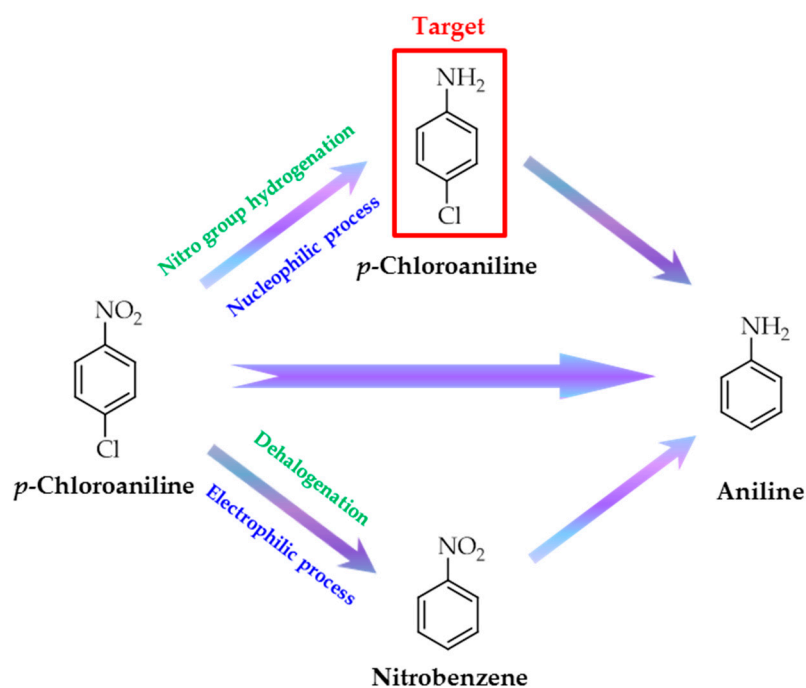


Figure 1. Main pathways associated with the selective hydrogenation of *p*-CNB (*p*-chloronitrobenzene).

Palladium immobilized catalysts with inorganic supports have good mechanical properties and durability. Such catalysts can be used on a large scale in industry. Gamma aluminum oxide (γ -Al₂O₃) has a perfect specific surface area and structural strength [20]. Moreover, the acid-base character of alumina materials has been appeared to enhance activation of H₂ on the supported transition element [21]. Poly(Styrene-*co*-maleic anhydride) polymer (SMA) is an important functional polymer, as the anhydride groups on SMA can react with different reagents such as alcohols, amines, or water to produce versatile derivatives [22]. By combining inorganic γ -Al₂O₃ and organic polymer together, a new organic-inorganic hybrid composite can be synthesized and applied as a catalyst support, which makes it accessible to distribute noble metal nanoparticles on its surface, which behave as excellent catalysts [23,24].

Here, we prepared a modified polymer-anchored palladium/ γ -Al₂O₃ pellet catalyst. SMA is directly encapsulated on the γ -Al₂O₃ pellet surface through polymerization. After being treated with ammonia water, amino-SMA (ASMA) material can be acquired as maleic anhydride, which can be hydrolyzed to yield carboxylic acid and primary amide [25]. Palladium species are supported on the organic-inorganic hybrid material. Then morpholine is used as a post-treatment reagent to attach onto the catalyst surface. The material as prepared was characterized by BET (BET surface area analyzer), XRD (X-ray diffraction), TGA (Thermal Gravimetric Analyzer), SEM (scanning electron microscope), TEM (Transmission electron microscope), FT-IR (Fourier Transform Infrared Spectrometer), and

ICP-OES (Inductively Coupled Plasma Optical Emission Spectrometer). We use this composite as an efficient heterogeneous catalyst in the selective hydrogenation of *p*-CNB to *p*-CAN. The catalyst showed very high selectivity and high conversion.

2. Results and Discussion

2.1. Catalyst Characterization

XRD patterns of catalyst samples are shown in Figure 2. Compared with the γ -Al₂O₃ pellets encapsulated with ASMA, intensities of the diffraction peaks of the samples after loading with palladium decrease obviously, which might be caused by the changes in the charge distribution and electrostatic field because of the existence of palladium nanoparticles and interaction with the surface of support [26]. The characteristic peaks at 40.2° and 46.8° can be attributed to the (111) and (200) planes of Pd, respectively [27]. However, the supports treated with ASMA encapsulation and morpholine modification did not show significant changes of crystallinity. This suggested that the crystallinity of the catalyst as prepared is mainly attributed to the property of original supports. Moreover, according to the Scherrer analysis on the basis of the XRD results, the mean sizes of Pd nanoparticles in the material before being treated with inhibitor was 28.50 nm, while it decreased to 25.61 nm after immersing in morpholine. Besides, the blank sample without ASMA polymer layer showed no specific peaks of Pd species after loading with 0.27 wt % Palladium measured by ICP-OES, which may be explained by the well dispersion of Palladium nanoparticles into the original pores of γ -Al₂O₃ pellets, in accordance with the reports on the Palladium catalysts with metal organic frameworks as supports [28].

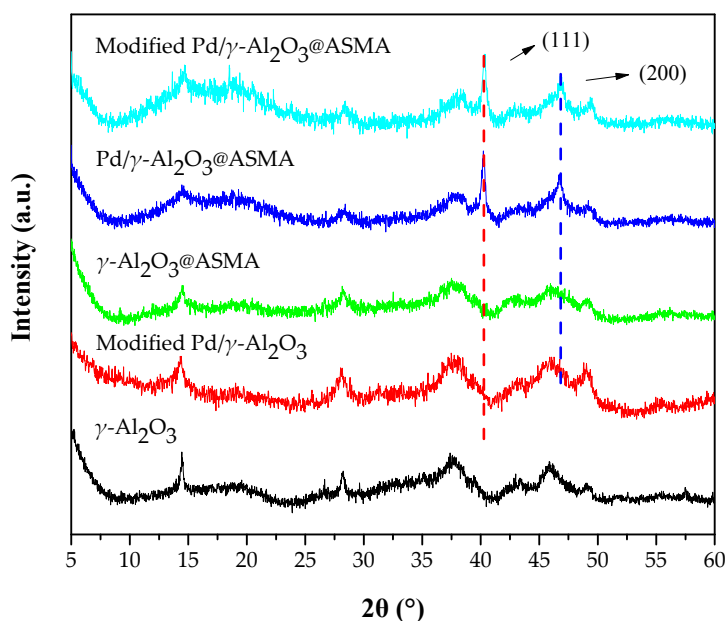


Figure 2. XRD (X-ray diffraction) patterns of catalyst and intermediates.

As presented in Figure 3, the modified ASMA polymers maintain sufficient thermal stability within 200 °C, even though a negligible inclination was observed. From 200 to 400 °C, the curve is slightly decreased, which may be due to the removal of surface-adsorbed species. Then, it is obvious that the quality of polymer rapidly declines at 400 °C. This should be attributed to the decomposition of polymer. Moreover, according to the data from TGA, the mass ratio of the ASMA polymer could be about 15.26% of modified Pd/γ-Al₂O₃@ASMA catalyst. From the TGA result, it could be strongly evident that the organic-inorganic hybrid material is a perfect candidate with high thermostability.

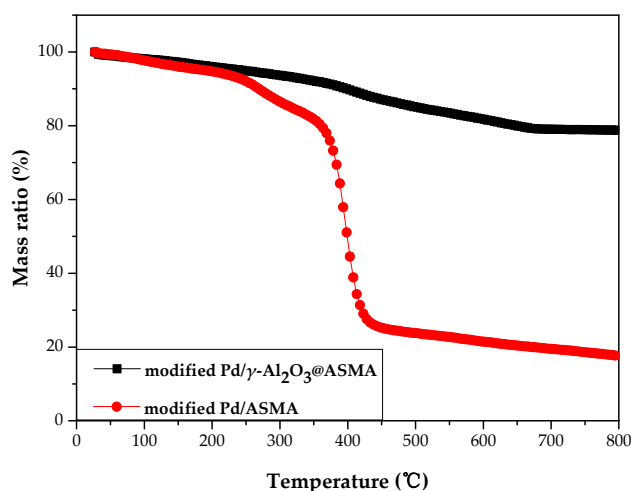


Figure 3. Thermogravimetric analysis (TGA) curves of modified Pd/ γ -Al₂O₃@ASMA (black) and modified Pd/ASMA (red). ASMA: amino poly (styrene-*co*-maleic anhydride).

SEM image of catalyst samples are presented in Figure 4. Compared with the SEM image of γ -Al₂O₃, which is encapsulated with ASMA, the channels of the blank γ -Al₂O₃ are more explicit and have more abundant pores. When the polymer is covered on the surface of the support, the morphology of γ -Al₂O₃ support is obviously changed and the dimension of channels on the support increased. However, after being loaded with PdCl₂ and post-treated with morpholine, the sample's morphology (especially the channels' dimensions) changes slightly. It is unambiguous to manifest that the polymer was uniformly covered on the macroporous alumina spheres after polymerization, and the post-treatment to obtain modified Pd/ γ -Al₂O₃@ASMA cannot transform the perfect porosity of original support. Such specific advantage guarantees this modified material as an efficient meso/macro-porous supportive candidate, and makes it possible to load Pd metal stably on the carrier surface [29].

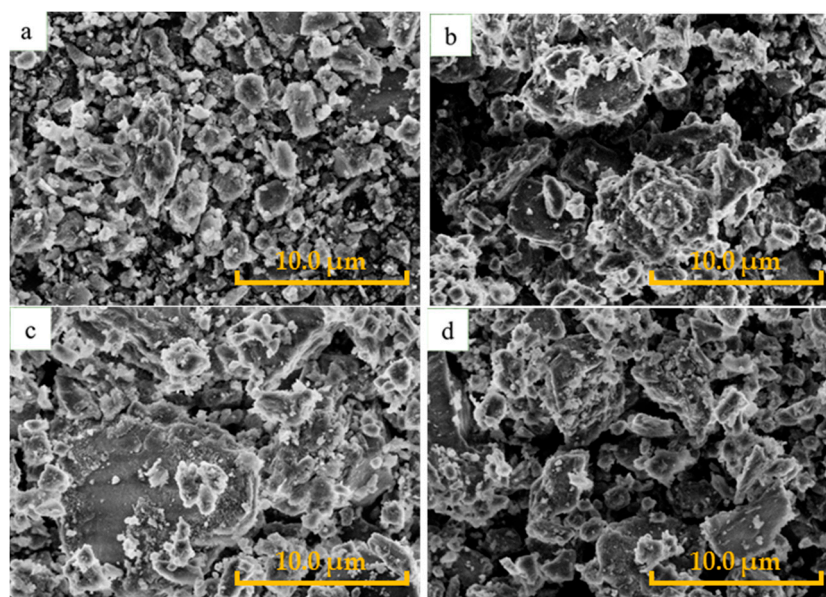


Figure 4. Scanning electron microscope (SEM) image of γ -Al₂O₃ (a); γ -Al₂O₃@ASMA (b); Pd/ γ -Al₂O₃@ASMA (c); and modified Pd/ γ -Al₂O₃@ASMA (d). The scale bar for all images is 10.0 μ m.

The nitrogen adsorption–desorption isotherm and the corresponding pore size distribution curve for Pd/ γ -Al₂O₃@ASMA catalyst and modified Pd/ γ -Al₂O₃@ASMA catalyst are shown in Figure S1. The N₂ adsorption–desorption isotherm of Pd/ γ -Al₂O₃@ASMA catalyst and modified Pd/ γ -Al₂O₃@ASMA catalyst showed type V curve with an obvious hysteresis in the desorption branch. The hysteresis loops on adsorption isotherms are relatively large, and the desorption curve is steeper than the adsorption curve. The persistence loops of adsorption and desorption isotherms satisfy the H₂ classification of IUPAC (International Union of Pure and Applied Chemistry) and such loops exhibit the mesoporous structure of the modified Pd/ γ -Al₂O₃@ASMA catalyst. Moreover, as revealed from Table 1, the pore volume, specific surface area, and pore size decreased drastically because of the loading of Pd metal. After the polymer is formed on the γ -Al₂O₃, the specific surface area changes slightly, and the pore volume as well as the pore size increase obviously. However, the pore volume (from 0.132 cm³/g to 0.066 cm³/g) and specific surface area (from 145.13 m²/g to 62.34 m²/g) of the catalyst were reduced up to half after the modification of morpholine, while the average pore diameter remained constant with 2.41 nm. A contributing factor may be that the modified catalyst did not block the pore throat position of the catalyst. After modification, the pore throat ratio of the catalyst remained constant, so that the pore size and the pore structure of the catalyst remained unchanged. At the same time, the presence of morpholine on the surface of sample decreased the adsorption property to nitrogen. Based on the result of TEM shown on Figure S2, the size of Pd before and after modification remained almost same (before modification: 28.36 nm; after modification: 26.11 nm). This supports the claim that the modification can only affect directly the surface of γ -Al₂O₃@ASMA material. Furthermore, from the TEM results, it can match the mean sizes of Pd nanoparticles acquired through the XRD results based on the Scherrer equation with slight deviation.

Table 1. Brunauer-Emmett-Teller (BET)-surface area, pore size, and pore volume of supports and catalysts.

Material	SA _{BET} ^a (m ² /g)	PD _{avg} ^b (nm)	PV _{total} ^c (cm ³ /g)
γ -Al ₂ O ₃	231.31	4.83	0.318
γ -Al ₂ O ₃ @ASMA	232.98	5.82	0.429
Pd/ γ -Al ₂ O ₃ @ASMA	145.13	2.41	0.132
Modified Pd/ γ -Al ₂ O ₃ @ASMA	62.34	2.41	0.066

^a Surface area (BET); ^b Average pore diameter (BJH); ^c total pore volume. BJH: Barrett-Joyner-Halenda pore-size distribution.

FT-IR results of catalysts as prepared are shown in Figure 5. The aromatic C–H stretching is located at 3026 cm^{−1}. The characteristic absorption band at 1711 cm^{−1}, is assigned to the carbonyl stretching vibration modes of maleimide [30]. The presence of para-substituted benzene was confirmed at 1450 cm^{−1}. In the FT-IR spectrum of catalyst immersed into morpholine, two new peaks are observed at 1106 cm^{−1} and 1635 cm^{−1}, attributed to the stretching vibration of –C–O–C– bond and tertiary amide. The existence of tertiary amide indicates that the morpholine sample can connect to the surface of polymer layer with a strong chemical bond resulting from the formation of amide [31], and the electron-rich –C–O–C– bond can still exist after modification.

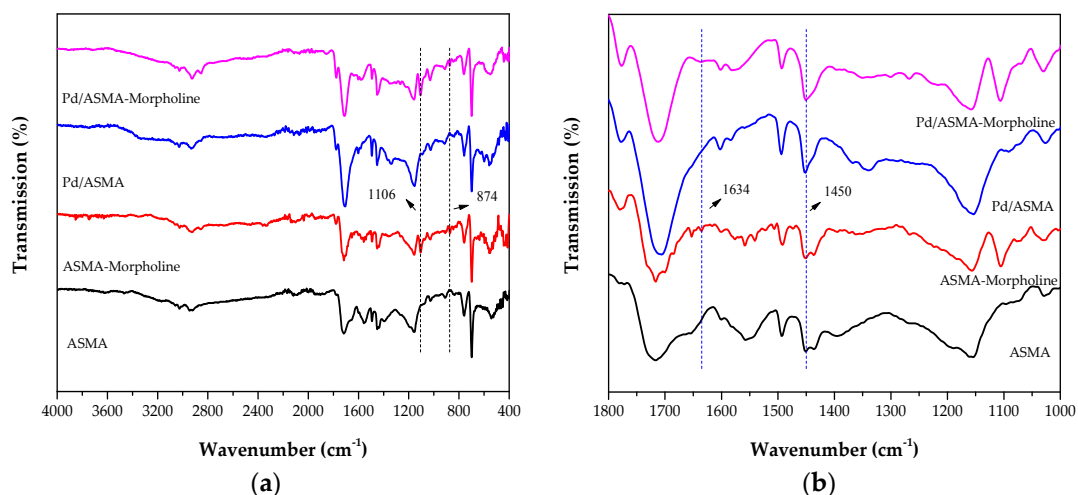


Figure 5. Infrared spectra of ASMA samples of pure sample (black), modified with morpholine (red), loaded with Pd (blue), and loaded with Pd after being modified with morpholine (magenta) recorded at room temperature, showing the range of (a) 4000–400 cm^{-1} and (b) 1800–1000 cm^{-1} .

2.2. Catalytic Activity

The catalytic properties of the modified $\text{Pd}/\gamma\text{-Al}_2\text{O}_3\text{@ASMA}$ catalysts obtained were systematically evaluated in the catalytic hydrogenation of *p*-CNB to *p*-CAN in a high-pressure reactor. In the process of hydrogenation, aniline is the main byproduct due to the unavoidable dehalogenation. Therefore, the conversion of reactant and selectivity of product *p*-CAN are significant [12]. In this research, the catalytic activity was performed by taking the equal amount of modified $\text{Pd}/\gamma\text{-Al}_2\text{O}_3\text{@ASMA}$ catalyst in the hydrogenation process with different Pd loading amount to investigate the influence of Pd loading ratio. In order to simplify the analysis, the amount of catalyst and substrate were taken in equal quantity (1 g of each) in the reaction.

According to the measurement with ICP-OES, the Pd contents in different catalysts were varied from 0.14 to 2.12 wt %. From Table 2, it can be observed that the conversion of *p*-CNB and selectivity of *p*-CAN on 0.27 wt % modified $\text{Pd}/\gamma\text{-Al}_2\text{O}_3\text{@ASMA}$ is the best, rather than other analogues under the same reaction conditions. The *p*-CAN selectivity can reach to 99.51%, while the *p*-CNB conversion is 99.74%. Based on the SEM, the polymer formed on the surface could enlarge the pore dimension obviously. It can be confirmed by the N_2 adsorption result. The pore dimensions increase from 4.83 to 5.82 nm, and this could be beneficial to the mass transferring in the process of hydrogenation. The high selectivity of *p*-CAN could indicate that the existed morpholine improves the tendency to weaken the dehalogenation efficiently.

Table 2. Catalytic properties of catalyst with different Pd loading.

Pd Loading (wt %)	Conversion (%)	Selectivity (%)
0.14	84.62	100
0.27	99.74	99.51
0.53	92.38	91.30
1.06	94.77	80.22
2.12	98.82	71.52

Reaction conditions: 1 g catalyst treated with 100 g/L morpholine, 1 g *p*-CNB dissolved in 50 mL ethanol, 80 °C, 600 rpm, and 2 MPa H_2 pressure in a 100 mL autoclave.

Figure 6 represents the relationship between the catalytic property of hydrogenation and reaction time. The conversion of reactant rises conspicuously as time increases until time reaches 4 h. After that, the substrate has reacted completely and almost all of *p*-CNB has transformed into *p*-CAN at 4 h.

Further, the target product could change to the byproduct because of the excessive hydrogenation, which manifests the declination of selectivity of target *p*-CAN [32].

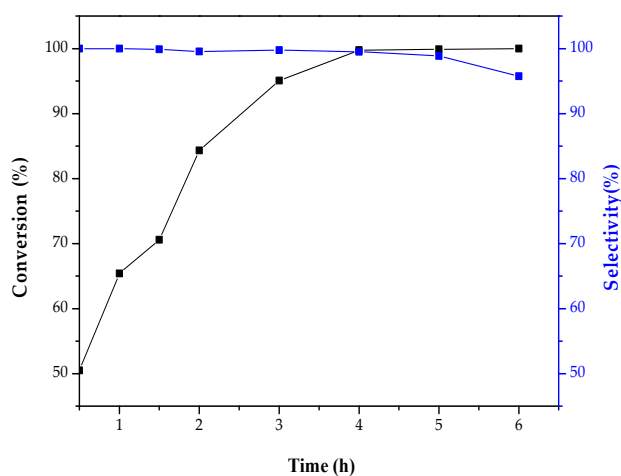


Figure 6. Impact of reaction time on the conversion (black) and selectivity (blue) in the selective hydrogenation of *p*-CNB. Reaction conditions: 1 g 0.27 wt % modified Pd/ γ -Al₂O₃@ASMA treated with 100 g/L morpholine, 1 g *p*-CNB dissolved in 50 mL ethanol, 80 °C, 600 rpm, and 2 MPa H₂ pressure in a 100 mL autoclave.

When the hydrogen pressure is increased from 0.5 to 2 MPa, the conversion rate is rapidly increased in *p*-CNB hydrogenation process (Figure 7). It is clear that the increase of hydrogen pressure leads to the enhancement of conversion. Beyond the 2 MPa hydrogen pressure, there is no significant influence on the experiment. Almost 100% selectivity of the products remains constant throughout the reaction under increasing hydrogen pressures up to 4 MPa. However, a higher pressure of hydrogen may be risk of explosion for the reactor and, further, it would enhance the cost of production.

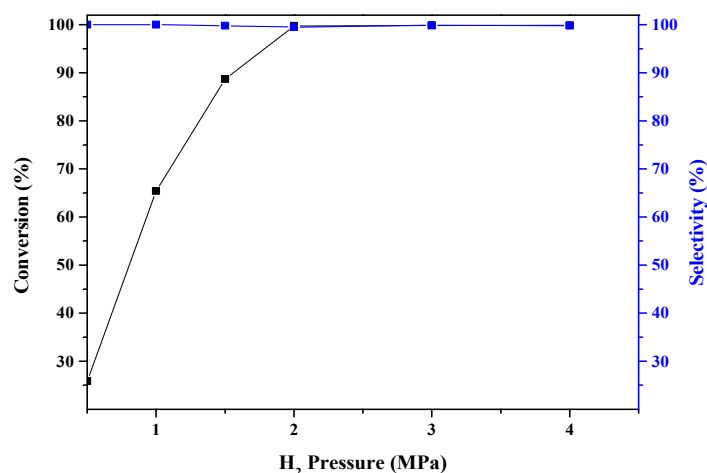


Figure 7. Impact of reaction pressure on the conversion (black) and selectivity (blue) in the selective hydrogenation of *p*-chloronitrobenzene (*p*-CNB). Reaction conditions: 1 g 0.27 wt % modified Pd/ γ -Al₂O₃@ASMA treated with 100 g/L morpholine, 1 g *p*-CNB dissolved in 50 mL ethanol, 80 °C, 600 rpm, and 4 h in a 100 mL autoclave.

As shown in Figure 8, the temperature has a remarkable effect on *p*-CNB selective hydrogenation. The result shows that the increase of temperature up to 80 °C leads to the improvement of conversion and selectivity, and then selectivity drastically decreases while the conversion remains steady. At 80 °C,

the conversion of *p*-CNB hydrogenation and the *p*-CAN selectivity reach almost 100%. During the reaction, *p*-CNB hydrogenation is a multi-step process. In this hydrogenation reaction, there is possibility of different pathways for generating the target product or byproduct. Such possibility is controlled by the attacking rate on the C-Cl bond or the N=O bond. After the formation of target product *p*-CAN, there could be further hydrogenation to produce aniline under high temperature.

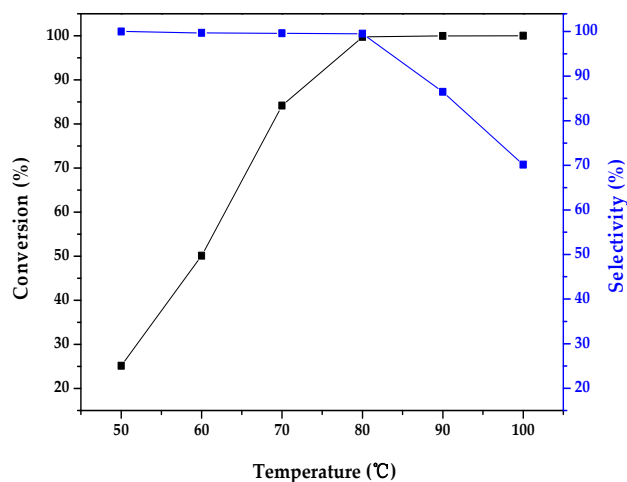


Figure 8. Impact of reaction temperature on the conversion (black) and selectivity (blue) in the selective hydrogenation of *p*-CNB. Reaction conditions: 1 g 0.27 wt % modified Pd/ γ -Al₂O₃@ASMA treated with 100 g/L morpholine, 1 g *p*-CNB dissolved in 50 mL ethanol, 600 rpm, 2 MPa H₂ pressure, and 4 h in a 100 mL autoclave.

The effects of agitation speed also alter on catalytic conversion and selectivity of *p*-CNB hydrogenation (Figure 9). The result shows that the increasing stirring rate leads to the improvement of conversion. The rate of conversion and selectivity raised abruptly when stirring rate increased from 200 rpm to 600 rpm. However, after 600 rpm, both of these parameters described above, remain almost stable. It is reasonable that, at lower stirring rate, the formation rate of target products is somewhat slower than the side reaction due to the inefficient mixing and the hindrance which decelerates the diffusion of H₂ gas into the liquid phase.

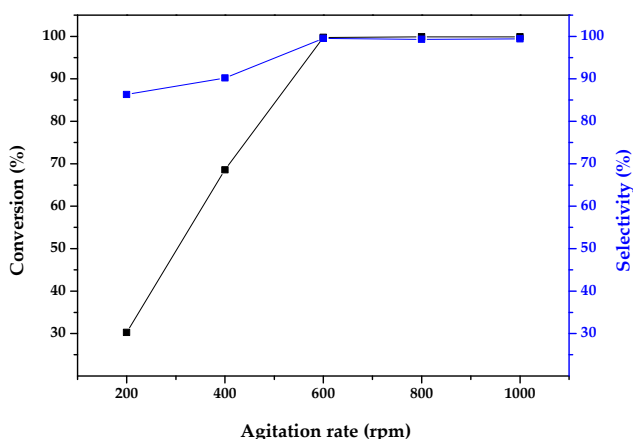


Figure 9. Impact of reaction stirring rate on the conversion (black) and selectivity (blue) in the selective hydrogenation of *p*-CNB. Reaction conditions: 1 g 0.27 wt % modified Pd/ γ -Al₂O₃@ASMA treated with 100 g/L morpholine, 1 g *p*-CNB dissolved in 50 mL ethanol, 80 °C, 2 MPa H₂ pressure, and 4 h in a 100 mL autoclave.

Taking into account the morpholine's effect on catalysts, different concentrations of morpholine were investigated under the same conditions (Figure 10). The result manifests that in the beginning, the increase of morpholine concentration up to 10 g/L raises the conversion rate slightly. From TEM and XRD characterization results, it can be explained that the nanoparticles' mean size decreased slightly, which could increase the surface of active metal nanoparticles. However, above this concentration, the conversion rate declined marginally up to 150 g/L, and above this concentration the conversion rate decreased abruptly. However, the yield of *p*-CAN is maximum at 100 g/L (*p*-CAN selectivity was 99.51%), and then decreases drastically with the addition of morpholine concentration. It indicates that morpholine has a good inhibitory effect on dechlorination when the concentration is less than 100 g/L, while the catalyst activity decreases significantly with the further addition of morpholine.

The stability and reusability of the modified Pd/ γ -Al₂O₃@ASMA catalyst are key factors in our research to determine it as an excellent candidate in the liquid heterogeneous hydrogenation of *p*-CNB to *p*-CAN. From the result depicted on Figure 11, the Pd catalyst as prepared can be easily recovered by filtration and reused in the hydrogenation at least 10 times without significant loss of its yield (considering the activity and selectivity). It indicates that the catalyst could maintain a high stability and avoid leaching of Pd nanoparticles, and it is also verified by the SEM characterization (Figure 4c,d). According to the characterization described above, during the procedure of catalysts preparation, the SMA polymer shell is uniformly coated on the surface of the alumina skeleton and the catalytic precursor Pd²⁺ could strongly bind with an electron donating group on the carrier's surface. After reduction, palladium clusters are uniformly embedded in the pores to improve stability [12]. Moreover, it can also exhibit that the morpholine species have a strong binding with the carrier, and the modification is unexpectedly efficient in the selective hydrogenation of *p*-CNB. All of these results can consistently account for the high catalytic activity, selectivity, and excellent reusability of modified 0.27 wt % Pd/ γ -Al₂O₃@ASMA catalyst.

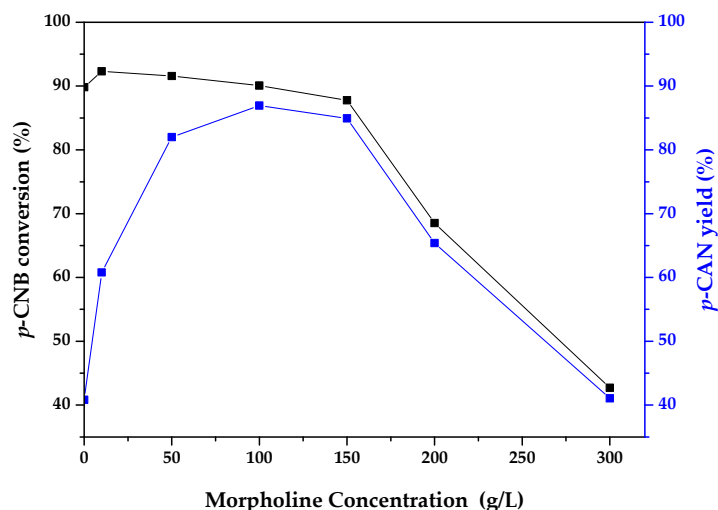


Figure 10. Impact of morpholine concentration on the conversion (black) and selectivity (blue) of catalytic hydrogenation of *p*-CNB. Reaction conditions: 1 g catalyst, 1 g *p*-CNB dissolved in 50 mL ethanol, 80 °C, 600 rpm, 2 MPa H₂ pressure, and 4 h in a 100 mL autoclave.

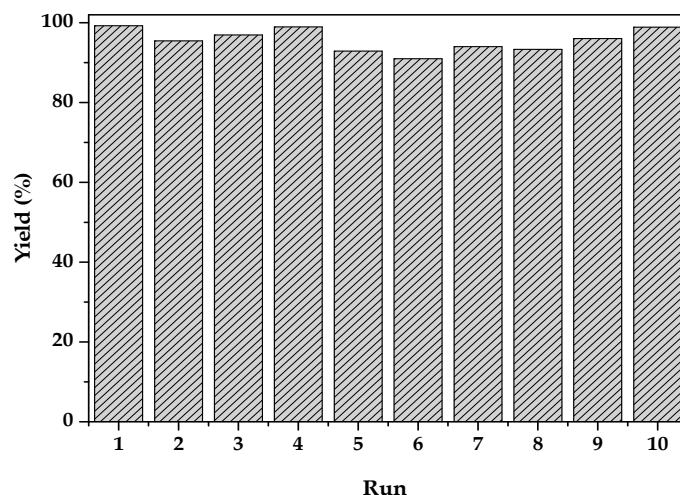


Figure 11. Investigation of catalyst's stability using 1 g modified 0.27 wt % Pd/ γ -Al₂O₃@ASMA catalysts. Reaction conditions: 100 g/L morpholine modified, 1 g *p*-CNB dissolved in 50 mL ethanol, 80 °C, 600 rpm, 2 MPa H₂ pressure, reaction time: 4 h.

2.3. Catalytic Mechanism Discussion

During the process of hydrogenation, the additive morpholine acts a significant role in the selective hydrogenation of *p*-CNB to *p*-CAN [33]. Based on the previous description of characterization, it can be declared that the morpholine is tightly bonded with the ASMA polymer, which can be verified by FT-IR characterization in Figure 4. In hydrogenation process, the hydrogen gas molecules firstly adsorbed on the surface of catalyst due to the Pd nanoparticles embedded on the surface and then splitted into activated hydrogen atoms [34], which could further react with the nitro group on *p*-CNB by nucleophilic reaction [35]. The lone-pair electrons that existed on oxygen atoms of morpholine could act as an induced target. These outward-pointed electron-rich species could provide repulsive force to restrict the adsorption of halogen side of *p*-CNB on the surface of catalyst, because the electronegativity of chlorine is higher than the oppositely oriented nitro group [36]. This performance of modified catalyst avoids electrophilic reaction (i.e., dehalogenation), which could sharply improve the selectivity of target product *p*-CAN (Figure 12).

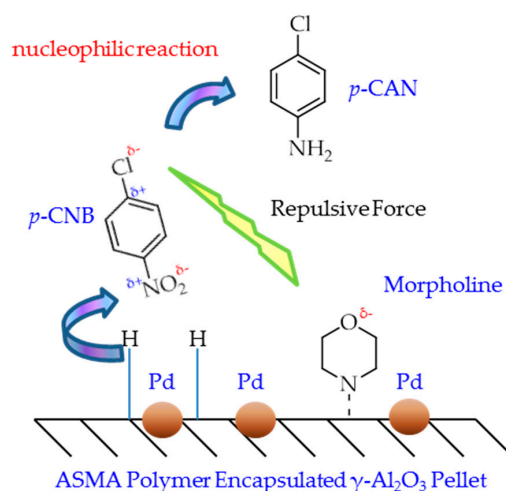


Figure 12. Scheme showing the principle of the catalyst composed of Pd-modified, ASMA polymer-encapsulated γ -Al₂O₃ pellet and the process of hydrogenation of *p*-CNB to *p*-chloroaniline (*p*-CAN).

In comparison, the blank sample without ASMA polymer layer (morpholine modified 0.27 wt % Pd/ γ -Al₂O₃) displays a significant loss of activity after being reused in the hydrogenation in 2nd and 3rd run, yet almost all the reactant *p*-CNB has transformed completely (Figure 13). The yield of *p*-CAN decreases to only 15.34% in the third run, while the yield of target using catalyst with ASMA layer could keep in more than 90%. This result solidly verifies that morpholine bonds on the ASMA layer because it cannot react with alumina to form a stable chemical bond. Thus, the leaching of morpholine in pure Al₂O₃ blank support counterpart can easily take place during the process of hydrogenation reaction, although the XRD result showed that Pd nanoparticles can disperse well on the surface of γ -Al₂O₃.

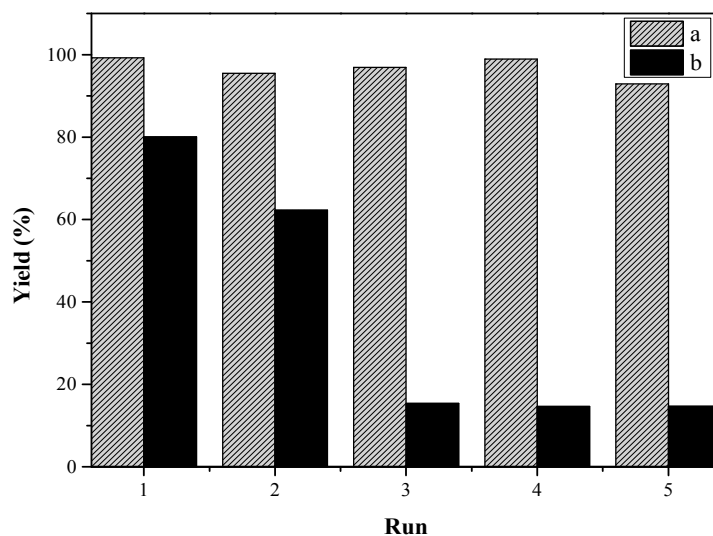


Figure 13. Reusability of (a) 1 g 0.27 wt % modified Pd/ γ -Al₂O₃@ASMA and (b) 1 g 0.27 wt % Pd/Al₂O₃ catalysts impregnated by morpholine in the catalytic hydrogenation of *p*-CNB. Reaction conditions: 100 g/L morpholine modified, 1 g *p*-CNB dissolved in 50 mL ethanol, 80 °C, 600 rpm, 2 MPa H₂ pressure, reaction time: 4 h.

3. Materials and Methods

3.1. Catalyst Preparation

The γ -Al₂O₃ pellets (4 mm diameter) were purchased from Henan Soar Environmental Technology Company (Zhengzhou, China). Other remaining chemical reagents were purchased from Sinopharm Group Chemical Reagent Company (Shanghai, China) and Shanghai Lingfeng Chemical Reagent Company (Shanghai, China). Further, γ -Al₂O₃ pellets were pretreated in deionized water by ultrasound for 20 min. Then, samples were dried at 105 °C overnight for further usage. Styrene, maleic anhydride, divinylbenzene, and dibenzoyl peroxide were mixed in the molar ratio of 200:200:20:1, respectively, to obtain polymerization solution, in which methanol was added as pore-forming agent. The γ -Al₂O₃ pellets were immersed in the polymerization solution for 3 h. Afterwards, the pellets were removed from the mixed solution and drained completely until no liquid drops falling. Then, the post-treated pellets were purged with N₂ gas in the oven. With temperature-programmed heating, poly (styrene-*co*-maleic anhydride) polymer (SMA) was produced and encapsulated on the surface of γ -Al₂O₃. After ammonization, γ -Al₂O₃@ASMA pellets (support) can be constructed. To immobilize Pd (1.0% by weight) on γ -Al₂O₃@ASMA support, 17 mg of PdCl₂ was dissolved into 10 mL ethanol in a round bottom flask with stirring and the solution was added dropwise into 1 g of γ -Al₂O₃@ASMA sample and refluxed for 12 h with continuous stirring. The solution was evaporated slowly to remove solvent completely. The resulting solid was washed with hot ethanol, dried, and then reduced by

hydrogen. Finally, Pd/ γ -Al₂O₃@ASMA as prepared was transferred in a round bottom flask containing the ethanol solution of morpholine and heated mildly for modification.

3.2. Catalyst Characterization

Surface areas of samples were measured by using an ASAP 2020 analyzer (Micromeritics, Norcross, GA, USA). The samples were degassed at 120 °C for 4 h under vacuum prior to N₂ adsorption measurements. The specific surface area, pore diameters, and pore volumes of catalyst samples were determined from nitrogen adsorption isotherms measured at −196 °C as per Brunauer-Emmett-Teller (BET) method. Thermogravimetric analysis (TGA) curves were taken by a STA 449F3 instrument (NETZSCH, Selb, Germany) under nitrogen with a heating rate of 10 °C/min from 30 °C to 800 °C. The loading capacity of Pd was obtained by an Optima 2000DV inductively coupled plasma optical emission spectrometry (ICP-OES) (PerkinElmer, Waltham, MA, USA). The catalyst was introduced into nitrate aqueous solution and heated at 50 °C until the PH value remained consistent, in order to digest the Pd supported on the γ -Al₂O₃ pellet. Fourier transform infrared (FT-IR) spectra (ALPHA-Bruker, Bruker, Germany) of the samples were recorded on an ALPHA FT-IR spectrophotometer (Bruker) in the range of 400–4000 cm^{−1}. Transmission electron microscopy (TEM) (JEOL, Tokyo, Japan) measurements were conducted with a JEOL JEM 2010 instrument with accelerating voltage of 200 KV. X-ray diffraction (XRD) patterns were recorded on a Rigaku Smartlab diffractometer (Rigaku, Tokyo, Japan) using Cu K α radiation (λ = 1.542 Å) operated at 40 kV and 100 mA. The sample of catalysts was examined by a S-4800 II field emission scanning electron microscope (FESEM) (Hitachi, Tokyo, Japan).

3.3. Hydrogenation of *p*-CNB Procedure

The catalytic hydrogenation reaction was carried out in a 100 mL stainless autoclave equipped with stirrer. Here, 1 g of catalyst, 1 g of *p*-CNB, and 50 mL of ethanol as solvent were added into the reactor. Hydrogen was repeatedly purged into the reactor at room temperature up to a pressure of 2 MPa to evacuate air. The reactor was heated to the required temperature, i.e., 80 °C, and then pressurized with hydrogen up to 2 MPa. Finally, the reaction was kept for 2 h with stirring at 600 rpm. After reaction was completed, the resulting filtrate sample mixture obtained by filtration was analyzed by GC [Agilent 6890 N equipped with a programmed split/splitless inlet, a flame ionization detector (FID), and a capillary column (HP-5, 30 m \times 0.32 mm \times 0.25 μ m, J&W Scientific)] (Agilent, Santa Clara, CA, USA). Additionally, the reaction conditions with respect to temperature, time, hydrogen pressure, stirring speed, amount of the catalyst loaded, and morpholine were optimized. In order to test the catalytic reusability of the modified Pd/ γ -Al₂O₃@ASMA, the catalyst, after being used, was separated by filtration, washed with ethanol, and dried in a vacuum desiccator at 120 °C, and then the recovered catalyst was reused in the next run reaction.

4. Conclusions

In summary, the performance of the supported Pd catalysts was monitored for the selective hydrogenation of *p*-CNB to *p*-CAN, and it was found that the support has a large effect on the catalyst activity and product selectivity. By combining with the amine functionalized poly (styrene-*co*-maleic anhydride) polymer and the alumina pellets, an organic-inorganic hybrid material was prepared to support palladium metal clusters (Pd/ γ -Al₂O₃@ASMA). The encapsulation of ASMA polymer layer could improve the porosity, which can automatically enhance the activity of reaction. After being immersed into morpholine, the FT-IR result verified the existence of surviving the C-O-C group on the polymer layer, and showed it can be responsible for the high selectivity of target products due to the induction effect. Moreover, compared with the counterpart catalyst without the encapsulated polymer (the modified Pd/Al₂O₃ catalyst), the developed modified Pd/ γ -Al₂O₃@ASMA catalyst is a stable catalyst for the hydrogenation of *p*-CNB to *p*-CAN without loss of conversion activity (almost 100%) and selectivity (up to 99.51%) after recycling it even 10 times. This result indicates that there is

strong binding connection between the morpholine and polymer layers, as well as great potential for industrial applications.

Supplementary Materials: The following are available online at www.mdpi.com/2073-4344/7/10/292/s1, Figure S1: N₂ adsorption–desorption isotherms and pore size distributions, and Figure S2: HRTEM images and Metal particle size distribution images.

Acknowledgments: This work was supported by Jianliang Zhu's laboratory of Nanjing Tech University.

Author Contributions: Jianliang Zhu conceived and designed the experiments; Wei Wang and Wenlong Xu performed the experiments, analyzed the data, and composed the manuscript; Kedar Bahadur Thapa checked, edited, and revised the manuscript; Xiaorui Yang performed the TGA and TEM experiments and analysis; Liyan Zhu and Jinhua Liang contributed to the reagents/program management.

Conflicts of Interest: The authors declare no conflict of interest.

References

1. Zhao, B.; Chen, Y.-W. Hydrogenation of *p*-chloronitrobenzene on Mo, La, Fe, and W-modified NiCoB nanoalloy catalysts. *J. Non Cryst. Solids* **2010**, *356*, 839–847. [CrossRef]
2. Lin, M.H.; Zhao, B.; Chen, Y.W. Hydrogenation of *p*-Chloronitrobenzene over Mo-Modified NiCoB Nanoalloy Catalysts: Effect of Mo Content. *Ind. Eng. Chem. Res.* **2009**, *48*, 7037–7043. [CrossRef]
3. Westerterp, K.R.; Molga, E.J.; Gelder, K.B.V. Catalytic hydrogenation reactors for the fine chemicals industries. Their design and operation. *Chem. Eng. Process.* **1997**, *36*, 17–27. [CrossRef]
4. Pietrowski, M.; Wojciechowska, M. The origin of increased chemoselectivity of platinum supported on magnesium fluoride in the hydrogenation of chloronitrobenzene. *Catal. Today* **2011**, *169*, 217–222. [CrossRef]
5. Menini, C.; Park, C.; Brydson, R.; Keane, M.A. Low-Temperature (553 K) Catalytic Growth of Highly Ordered Carbon Filaments during Hydrodechlorination Reactions. *J. Phys. Chem. B* **2000**, *104*, 4281–4284. [CrossRef]
6. Liang, M.; Wang, X.; Liu, H.; Liu, H.; Wang, Y. Excellent catalytic properties over nanocomposite catalysts for selective hydrogenation of halonitrobenzenes. *J. Catal.* **2008**, *255*, 335–342. [CrossRef]
7. Cárdenas-Lizana, F.; Berguerand, C.; Yuranov, I.; Kiwi-Minsker, L. Chemoselective hydrogenation of nitroarenes: Boosting nanoparticle efficiency by confinement within highly porous polymeric framework. *J. Catal.* **2013**, *301*, 103–111. [CrossRef]
8. Zhang, Q.; Su, C.; Cen, J.; Feng, F.; Ma, L.; Lu, C.; Li, X. The Modification of Diphenyl Sulfide to Pd/C Catalyst and Its Application in Selective Hydrogenation of *p*-Chloronitrobenzene. *Chin. J. Chem. Eng.* **2014**, *22*, 1111–1116. [CrossRef]
9. Cárdenas-Lizana, F.; Gómez-Quero, S.; Amorim, C.; Keane, M.A. Gas phase hydrogenation of *p*-chloronitrobenzene over Pd–Ni/Al₂O₃. *Appl. Catal. A* **2014**, *473*, 41–50. [CrossRef]
10. Fan, G.-Y.; Huang, W.-J. Synthesis of ruthenium/reduced graphene oxide composites and application for the selective hydrogenation of halonitroaromatics. *Chin. Chem. Lett.* **2014**, *25*, 359–363. [CrossRef]
11. Beswick, O.; Lamey, D.; Muriset, F.; Lagrange, T.; Oberson, L.; Yoon, S.; Sulman, E.; Dyson, P.J.; Kiwi-Minsker, L. Ni-based structured catalyst for selective 3-phase hydrogenation of nitroaromatics. *Catal. Today* **2016**, *273*, 244–251. [CrossRef]
12. Fu, T.; Hu, P.; Wang, T.; Dong, Z.; Xue, N.; Peng, L.; Guo, X.; Ding, W. High selectivity to *p*-chloroaniline in the hydrogenation of *p*-chloronitrobenzene on Ni modified carbon nitride catalyst. *Chin. J. Catal.* **2015**, *36*, 2030–2035. [CrossRef]
13. Chen, T.; Li, D.; Jiang, H.; Xiong, C. High-performance Pd nanoalloy on functionalized activated carbon for the hydrogenation of nitroaromatic compounds. *Chem. Eng. J.* **2015**, *259*, 161–169. [CrossRef]
14. Chatterjee, M.; Ishizaka, T.; Kawanami, H. Preparation and characterization of PdO nanoparticles on trivalent metal (B, Al and Ga) substituted MCM-41: Excellent catalytic activity in supercritical carbon dioxide. *J. Colloid Interface Sci.* **2014**, *420*, 15–26. [CrossRef] [PubMed]
15. Kratky, V.; Kralik, M.; Mecarova, M.; Stolcova, M.; Zalibera, L.; Hronec, M. Effect of catalyst and substituents on the hydrogenation of chloronitrobenzenes. *Appl. Catal. A* **2002**, *235*, 225–231. [CrossRef]
16. Tu, W.; Cao, S.; Yang, L.; Wang, W. Modification effects of magnetic supports and bimetallic structures on palladium nanocluster catalysts. *Chem. Eng. J.* **2008**, *143*, 244–248. [CrossRef]

17. Cárdenas-Lizana, F.; Gómez-Quero, S.; Hugon, A.; Delannoy, L.; Louis, C.; Keane, M.A. Pd-promoted selective gas phase hydrogenation of *p*-chloronitrobenzene over alumina supported Au. *J. Catal.* **2009**, *262*, 235–243. [CrossRef]
18. Uflyand, I.E.; Ilchenko, I.A.; Sheinker, V.N.; Bulatov, A.V. Heterogenization of palladium(II) chelates on a sibunite. *Transit. Met. Chem.* **1991**, *16*, 293–295. [CrossRef]
19. Yu, Z.; Liao, S.; Xu, Y.; Yang, B.; Yu, D. Hydrogenation of nitroaromatics by polymer-anchored bimetallic palladium-ruthenium and palladium-platinum catalysts under mild conditions. *J. Mol. Catal. A Chem.* **1997**, *120*, 247–255. [CrossRef]
20. García-Diéguez, M.; Pieta, I.S.; Herrera, M.C.; Larrubia, M.A.; Malpartida, I.; Alemany, L.J. Transient study of the dry reforming of methane over Pt supported on different γ -Al₂O₃. *Catal. Today* **2010**, *149*, 380–387. [CrossRef]
21. Skotak, M.; Karpinski, Z.; Juszczak, W.; Pielaszek, J.; Kepinski, L.; Kazachkin, D.; Kovalchuk, V.; Ditrí, J. Characterization and catalytic activity of differently pretreated Pd/Al₂O₃ catalysts: The role of acid sites and of palladium–alumina interactions. *J. Catal.* **2004**, *227*, 11–25. [CrossRef]
22. Al-Sabagh, A.M.; El-Din, M.R.N.; Morsi, R.E.; Elsabee, M.Z. Demulsification efficiency of some novel styrene/maleic anhydride ester copolymers. *J. Appl. Polym. Sci.* **2008**, *108*, 2301–2311. [CrossRef]
23. Mishra, D.K.; Dabbawala, A.A.; Hwang, J.-S. Poly (styrene-*co*-divinylbenzene) amine functionalized polymer supported ruthenium nanoparticles catalyst active in hydrogenation of xylose. *Catal. Commun.* **2013**, *41*, 52–55. [CrossRef]
24. Hao, L.; Zhao, Y.; Yu, B.; Zhang, H.; Xu, H.; Xu, J.; Liu, Z. Polyurea-supported metal nanocatalysts: Synthesis, characterization and application in selective hydrogenation of *o*-chloronitrobenzene. *J. Colloid Interface Sci.* **2014**, *424*, 44–48. [CrossRef] [PubMed]
25. Duan, H.; Qiu, T.; Guo, L.; Ye, J.; Yuan, Y.; Li, X. The aminolysis of styrene–maleic anhydride copolymers for a new modifier used in urea-formaldehyde resins. *Int. J. Adhes. Adhes.* **2016**, *66*, 138–146. [CrossRef]
26. Plessers, E.; Fu, G.; Tan, C.; De Vos, D.; Roeflaers, M. Zr-Based MOF-808 as Meerwein–Ponndorf–Verley Reduction Catalyst for Challenging Carbonyl Compounds. *Catalysts* **2016**, *6*, 104. [CrossRef]
27. Kozell, V.; Giannoni, T.; Nocchetti, M.; Vivani, R.; Piermatti, O.; Vaccaro, L. Immobilized Palladium Nanoparticles on Zirconium Carboxy-Aminophosphonates Nanosheets as an Efficient Recoverable Heterogeneous Catalyst for Suzuki–Miyaura and Heck Coupling. *Catalysts* **2017**, *7*, 186. [CrossRef]
28. Zhao, X.; Jin, Y.; Zhang, F.; Zhong, Y.; Zhu, W. Catalytic hydrogenation of 2,3,5-trimethylbenzoquinone over Pd nanoparticles confined in the cages of MIL-101(Cr). *Chem. Eng. J.* **2014**, *239*, 33–41. [CrossRef]
29. Han, D.; Li, X.; Zhang, L.; Wang, Y.; Yan, Z.; Liu, S. Hierarchically ordered meso/macroporous γ -alumina for enhanced hydrodesulfurization performance. *Microporous Mesoporous Mater.* **2012**, *158*, 1–6. [CrossRef]
30. Vermeesch, I.; Groeninckx, G. Chemical Modification of Poly(styrene-*co*-maleic anhydride) with Primary N-alkylamines by Reactive Extrusion. *J. Appl. Polym. Sci.* **1994**, *53*, 1365–1373. [CrossRef]
31. Johnson, J.B.; Funk, G. Determination of carboxylic acid anhydrides by reaction with morpholine. *Anal. Chem.* **1955**, *27*, 1464–1465. [CrossRef]
32. Antonetti, C.; Oubenali, M.; Raspolli Galletti, A.M.; Serp, P.; Vannucci, G. Novel microwave synthesis of ruthenium nanoparticles supported on carbon nanotubes active in the selective hydrogenation of *p*-chloronitrobenzene to *p*-chloroaniline. *Appl. Catal. A* **2012**, *421*, 99–107. [CrossRef]
33. Baumeister, P.; Blaser, H.U.; Scherrer, W. Chemoselective Hydrogenation of Aromatic Chloronitro Compounds with Amidine Modified Nickel Catalysts. *Stud. Surf. Sci. Catal.* **1991**, *59*, 321–328.
34. Shen, J.-H.; Chen, Y.-W. Catalytic properties of bimetallic NiCoB nanoalloy catalysts for hydrogenation of *p*-chloronitrobenzene. *J. Mol. Catal. A Chem.* **2007**, *273*, 265–276. [CrossRef]
35. Coq, B.; Tijani, A.; Dutartre, R.; Figuéras, F. Influence of support and metallic precursor on the hydrogenation of *p*-chloronitrobenzene over supported platinum catalysts. *J. Mol. Catal.* **1993**, *79*, 253–264. [CrossRef]
36. Menini, C.; Park, C.; Shin, E.-J.; Tavoularis, G.; Keane, M.A. Catalytic hydrodehalogenation as a detoxification methodology. *Catal. Today* **2000**, *62*, 355–366. [CrossRef]

